



Developing a 3D mineral texture quantification method of drill core for geometallurgy

M.J. Voigt^{1,2}, J. Miller³, L. Bbosa¹, R.A. Govender⁵, D. Bradshaw⁴, A. Mainza¹, and M. Becker¹

Affiliation:

¹ Centre for Minerals Research, University of Cape Town, Rondebosch, South Africa

² Economic Geology Competency, Council for Geoscience, South Africa

³ Department of Earth Sciences, Stellenbosch University, Matieland, South Africa

⁴ Minerals to Metals Initiative, University of Cape Town, Rondebosch, South Africa

⁵ Blast Impact and Survivability Research Unit, University of Cape Town, Rondebosch, South Africa

Correspondence to:

M. Voigt

Email:

mvoigt@geoscience.org.za

Dates:

Received: 21 Jan. 2019

Revised: 15 Mar. 2019

Accepted: 26 Mar. 2019

Published: April 2019

How to cite:

Voigt, M.J., Miller, J., Bbosa, L., Govender, R.A., Bradshaw, D., Mainza, A., and Becker, M.

Developing a 3D mineral texture quantification method of drill core for geometallurgy.

The Southern African Institute of Mining and Metallurgy

DOI ID:

<http://dx.doi.org/10.17159/2411-9717/590/2019>

ORCID ID:

<https://orcid.org/0000-0003-2152-2070>

Synopsis

Mineral texture is a critical factor which controls ore variability and is an important attribute in geometallurgy. In relation to downstream processes, it affects the fracture pattern during breakage, where rock strength is inherently a function of mineral texture. Because of the subjective nature of mineral texture, it has not been easy to quantify, especially in the context of a measurement suitable for use in geometallurgical programmes. The aim of this paper is to present the first steps in developing a 3D mineral texture quantification method for drill core and to assess its sensitivity to differences in rock strength using a case study. The methodology includes classifying the textural information using the 3D grey level co-occurrence matrices (GLCM) and X-ray computed tomography (XCT) coupled method. Rock strength tests were performed using the split Hopkinson pressure bar (SHPB). The case study investigates a heterogeneous polymetallic sulphide deposit and a homogeneous shale subdivided into three 'mineral textural types'. The variability is largely captured by the GLCM matrices, and preliminary trends can be observed where the shale is finer grained and has a higher yield strength in comparison with the coarser grained polymetallic sulphide ore.

Keywords

drill core, mineral texture, ore variability.

Introduction

Modern mining requires the exploitation of lower grade and more complex, heterogeneous orebodies to address the growing industry demands. Historically, processing plants were designed and built based on average ore characteristics and therefore are relatively inflexible when facing the full spectrum of ore variability in heterogeneous orebodies (Lamberg, 2011; Lotter, 2011; Schouwstra *et al.*, 2013). The practice of geometallurgy represents an opportunity to manage ore variability in the mining industry (Powell 2013; Baum, 2014; Yildirim *et al.*, 2014; Nguyen, 2013). It focuses on quantifying the relationships between ore characteristics and their downstream mining and processing responses, often starting with small-scale laboratory testing. The purpose of geometallurgy is linked to maximizing the net present value (NPV) of an orebody by minimizing technical and operational risk – where 'ore variability' is considered one of the most significant technical risks.

A key parameter that constitutes ore variability is the heterogeneity in mineral texture, which further controls the response of the ore to processing (Schouwstra and Smit, 2011; Schouwstra *et al.*, 2013; Yildirim *et al.*, 2014; Lund; Lamberg, and Lindberg, 2013). Mineral texture summarizes not only the geometrical characteristics of a grain or particle (shape and size), but also includes interrelationships and compositions, *i.e.* mineralogy (Craig and Vaughan, 1994). Numerous examples occur in the literature describing how mineral texture affects downstream processing. For example, in comminution, texture influences rock strength, liberation, product particle size distribution, target grain size, and grindability of the ore (Vizcarra *et al.*, 2010; Lotter *et al.*, 2011; Ghorbani *et al.*, 2011, 2013; Nwaila, 2014; Evans, Wightman, and Yuan, 2015; Little *et al.*, 2016; McGrath, O'Connor, and Eksteen, 2015; Tungpalan *et al.*, 2015; Miller and Lin, 2016). In flotation, texture affects the potential mineral grade-recovery relationship (Gaspar and Pinto, 1991; Gottlieb *et al.*, 2000). In leaching, texture affects the accessibility of the valuable mineral to the lixiviant (Lui, Pawlik, and Laskowski, 2015; Maydagan *et al.*, 2016). Texture has also been used for the characterization and prediction of acid rock drainage (Parbhakar-Fox *et al.*, 2011).

The use of qualitative mineral texture descriptors involves some limitations, because the subjectivity of these descriptors then increases (Vos, 2016). In terms of mineral textural quantification, only aspects of quantified mineral texture (*e.g.* shape or size) are used, and therefore the observed relationships do not always hold because studies have not holistically defined the inherent geometrical and compositional

Developing a 3D mineral texture quantification method of drill core for geometallurgy

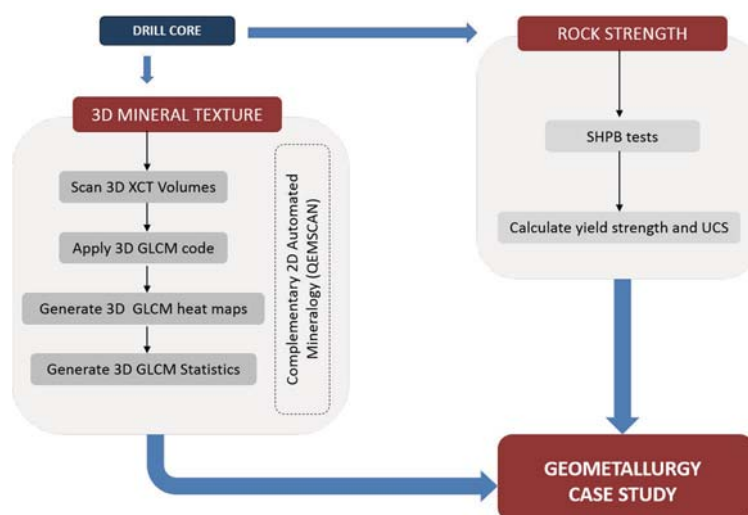


Figure 1—Summarized methodology for this study

variability of different geomaterials. Furthermore, most of these abovementioned studies focused on particulate samples, and therefore the method is not directly applicable to drill cores. More recent studies have therefore focused on developing methods to quantify mineral texture through automated textural pattern recognition on drill cores, as well as testing the potential to predict downstream mineral performance (Becker *et al.*, 2016). Perez-Barnuevo, Lévesquea, and Bazin, (2018) tested the link between texture and mineral behaviour during comminution and heavy liquid separation. They used a method that acquired the textural information through the Mineral Liberation Analyser (MLA), and coupled it with the grey level co-occurrence matrices (GLCM) and grey level run length matrices (GLRLM) for extraction and automated recognition of textural information in 2D. However, mineral texture measurements that are limited to 2D do not necessarily provide complete dimensions for grain characteristics (3D), which also further increases subjectivity. A potential method using X-ray computed tomography (XCT) coupled with 3D GLCM to achieve 3D mineral textural quantification was proposed by Jardine, Becker, and Miller (2018) and its potential as a small-scale geometallurgical test was demonstrated (Becker *et al.*, 2016) using a Ni-Cu sulphide ore. However, because the study used only one ore type, further studies are needed to fully understand the robustness of this method towards a variety of ore types and its suitability regarding downstream processes.

This paper further develops the method using XCT and 3D GLCM to quantify mineral texture in geometallurgy, where rock strength is a function of the inherent mineralogical and textural features of a rock (Olsson, 1974; Howarth and Rowland, 1987). Therefore, in order to demonstrate that the observed differences in mineral textures captured by the abovementioned method are meaningful, rock strength was also measured. The case studies include a heterogeneous polymetallic ore and a homogeneous shale to represent a different suite of mineral textural types as part of the ongoing research (Becker *et al.*, 2016; Jardine, Becker, and Miller, 2018).

Experimental procedure

As a proof of concept, three large pieces of samples (approx. 30 cm²) were used in this study. The first sample (sample A) is a relatively homogeneous, well characterized Malmesbury shale

from a quarry in Cape Town, South Africa (Bbosa, 2007; Hill *et al.*, 2018). The shale was used to develop the initial methodology. The other two rock types were sampled from a local polymetallic (Pb-Zn-Cu) sulphide ore deposit in South Africa (samples B and C). Three cylindrical diamond drill core sets with diameters of 13, 19, and 26 mm were obtained manually from each of the grab samples. The same drill cores were cut into a minimum of 15 pieces (discs) of equal length, which gave an overall 135 pieces for use in the proof of concept.

A subset of the pieces was visually selected and scanned by XCT using the NIKON XTH 225 ST system housed in the Microfocus X-ray Radiography and Tomography facility at the South African Nuclear Energy Corporation (Bam *et al.*, 2016). A constant set of XCT scan parameters was used: 175 kV, 15 µm voxel size, averaging of three frames, 1000 projections, using a 25 mm Cu filter, with approximately 20 minutes per scan. The approach for this study is consistent with the 3D GLCM and XCT method of Jardine, Becker, and Miller (2018). The grey level co-occurrence matrices were extracted from the XCT image stacks using the dedicated MATLAB script by Jardine, Becker, and Miller (2018). After XCT scanning, a subset of the same pieces was prepared into blocks for analysis on an FEI 650F FEG QEMSCAN at the University of Cape Town to determine the basic mineralogical characteristics of each sample. Samples were scanned using the field image analysis routine with instrument operating parameters of 25 kV, 10 nA, 357 fields/frames at a 15 µm pixel spacing. The methodology is summarized in Figure 1.

All rock strength tests were performed on the 135 pieces using the Blast Impact and Survivability Research Unit (BISRU) split Hopkinson bar facility in the Mechanical Engineering department at the University of Cape Town. High strain rate stress-strain responses of geomaterials can be measured through SHPB testing, which can characterize the strength of these materials by using common engineering parameters. SHPB testing was preferred over quasi-static testing, as the high strain rates applied during the SHPB test are more reflective of those encountered in a comminution or milling context. These tests followed the procedure outlined by Bbosa (2007) and Govender *et al.* (2012). After testing different strikers and conditions, the standard conditions for all impacts included using a conical striker (400 mm long, and a mass of 885 g), strain gauge bridge excitation voltage of 2 V, strain gauge amplifier gain of 1000, and

Developing a 3D mineral texture quantification method of drill core for geometallurgy

sampling rate of 10 megasamples per second (MSa/s). Three different pressures (using the pressure-controlled gas gun) were tested for every core size. The initial test methodology included testing the samples at the desired pressures of 220 (low), 280 (medium), and 400 kPa (high). A light trap and digital oscilloscope were used to measure the striker velocities for each impact, and hence calculate the kinetic energy for each collision. To facilitate dynamic equilibrium of the specimen as early as possible, pulse smoothing was applied in the form of masking tape between striker and input bar to tune the stress wave rise time. Furthermore, the SHPB data was calibrated by obtaining a constant proportionality constant directly related to the output voltage applied to the stress using one-dimensional theory (see Govender *et al.*, 2012). Calculations for the stress-strain data were done and the results plotted, and the data was used to calculate fracture properties. It should be noted that the data presented in this paper is only for the 13 mm drill core pieces at 220 kPa pressure, for direct comparison between the three mineral texture types.

Results

Initial ore characterization

The different 'mineral texture types' were identified through visual inspection of the different cores, and subsequently divided into shale and the two polymetallic ore samples on the basis of their variability in mineralogical composition as well as their geometrical differences (texture). The variability of these samples is illustrated through the selected hand specimens and QEMSCAN false-colour images in Figures 2 and 3, respectively. Sample A (shale) is a homogeneous (equigranular) fine-grained rock, with quartz, biotite, and feldspar as the dominant minerals. Samples B and C are medium-grained, heterogeneous magnetite rock. Sample B consists predominantly of magnetite and pyroxmangite, and its sulphide minerals are mostly chalcopyrite, and pyrrhotite. Sample C is predominantly quartz, magnetite and pyroxmangite, associated with sphalerite.

Quantification of mineral texture

2D slices extracted from the 3D volumes and the grey level XCT scans are illustrated in Figure 4 A1, B1, and C1 (respectively samples A, B, and C). The XCT images duplicate the basic textures, where sample A is fine-grained, and B and C are

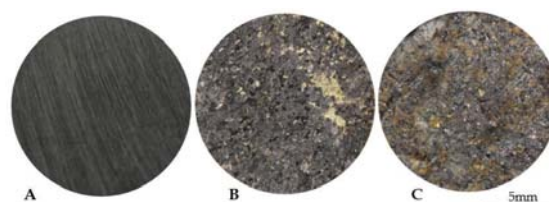


Figure 2—Photographs of the selected samples representing the three mineral texture types: (A) shale, (B) and (C) polymetallic Pb-Cu-Zn ore

medium-grained. The QEMSCAN analysis is further used as a supporting tool to interpret the mineralogy captured by the XCT images, since both the QEMSCAN backscattered electron (BSE) and XCT grey level images represent relative differences in mineral density (Figure 3 D, E, and F against Figure 4 A1, B1, and C1 respectively).

The brighter pixels within a grey level image (*e.g.* Figure 4 A1, B1, and C1) are related to the denser minerals (sulphides), whereas the darker pixels are related to the less dense minerals (quartz, biotite). As an example, the GLCM matrices (Figure 4 A2, B2, and C2) can be calculated based on the grey level information for a selected 2D XCT image extracted from the 3D (XCT) volume. The accompanying GLCM colour heat map distributions are also provided for each GLCM matrix (Figure 4 A3, B3, and C3) to reveal hidden information that is not easily visible to the naked eye. The matrices have two axes related to pixel pairs, where the vertical axis represents the reference pixel value and the horizontal axis represents its neighbouring pixel value (Jardine, Becker, and Miller, 2018).

For the selected XCT slice, the shale (sample A) has a GLCM distribution which is limited to the top left (low-density) quadrant and records no information in the bottom right (high-density) quadrant. The distribution for polymetallic sulphide sample B is also restricted to the top left quadrant (note the absence of sulphides in this particular XCT slice, chosen rather to illustrate differences in grain size distribution). The difference between these two distributions is in the width of the matrices. Sample A has a broader distribution than sample B. Sample C has peaks in both quadrants, and has a narrow distribution similar to B. The narrow *versus* broader distributions are indicative of the variation in grain sizes (Jardine, Becker, and Miller, 2018).

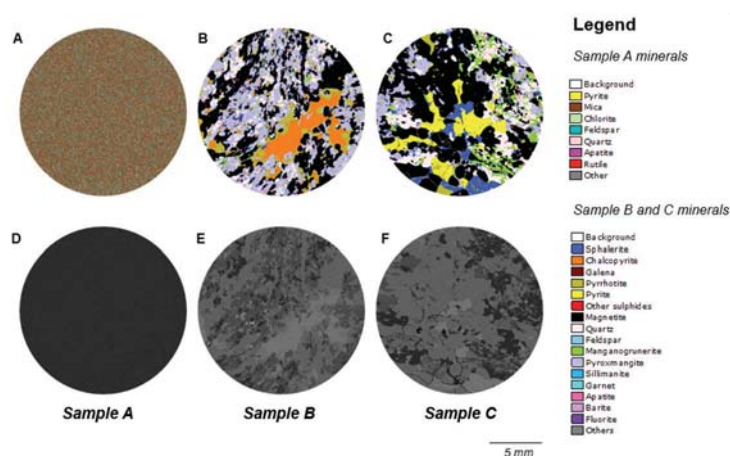


Figure 3—QEMSCAN false-colour images of the three rock samples (A shale, B and C polymetallic ore) accompanied by their corresponding backscattered electron images (D, E, F)

Developing a 3D mineral texture quantification method of drill core for geometallurgy

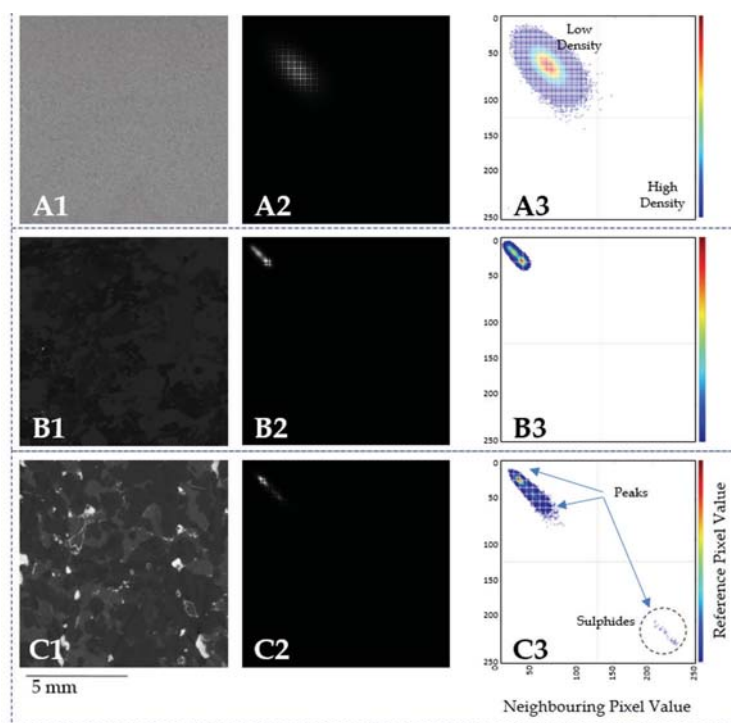


Figure 4—2D XCT images can be extracted from the 3D volumes (A1, B1, C1) and examples are given for the shale (A1) and the polymetallic ore sample B (B1) and sample C (C1). Each XCT image (input) is accompanied by its GLCM matrix (A2, B2, C2 for samples A, B, and C respectively), which summarizes the mineral textural information of the spatial relationship between the grey values within the XCT images (output). The 'colour intensity' heat map further reveals the hidden information which may not be visible to the naked eye (A3, B3, and C3 for each of the samples) and enhances the information on the mineralogical and textural variability for each of the matrices

The broader (sample A) distribution is indicative of a fine-grained material, and the narrower distributions (samples B and C) are indicative of a coarser grained material such as the medium-grained texture for these polymetallic ore samples. The peaks in the quadrants indicate the grey level peaks of either the silicate or BMS/oxide minerals. The sensitivity in the mineralogy can therefore be seen in either the top left quadrant (low-density minerals) or the bottom right quadrant (high-density minerals). For example, sample A is dominated by low-density silicate minerals and has one dominant peak in the top left quadrant, whereas, sample C consists of silicates, oxides, and sulphides, and therefore three peaks can be seen. Two of the peaks are in the low-density quadrant and the third peak is in the bottom right quadrant (representing the sulphide population).

The image information for the entire 3D volumes can be converted to numerical information using statistical descriptors provided by Haralick, Shanmugam, and Dinstein (1973) and the script adaptation by Jardine, Becker, and Miller (2018). The four

statistical descriptors that link to mineralogy and texture are homogeneity, contrast, correlation, and energy. These descriptors are essentially variability in the grey level information as well as the spatial distribution of these grey levels in relation to each other (Haralick, Shanmugam, and Dinstein, 1973). Homogeneity and contrast refer to the number of grey level transitions and the

Sample	N (2D images)	Minimum	Maximum	Mean
Sample A	100	70 298	70 549	70 385
Sample B	98	68 487	71 375	69 315
Sample C	98	71 004	75 380	74 128

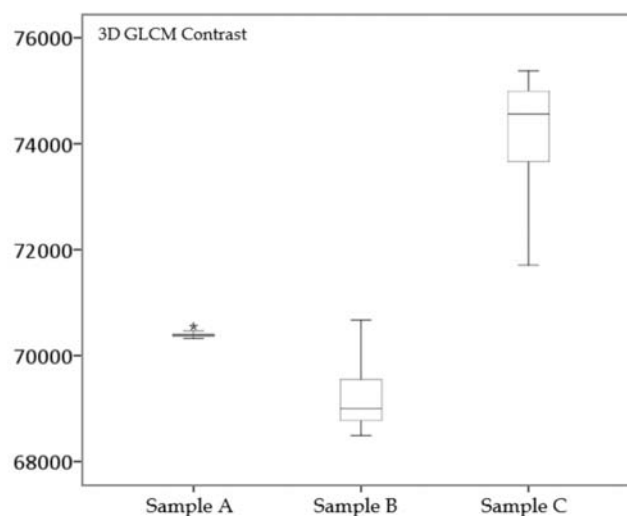


Figure 5—Box-and-whisker plot summarizing the 3D GLCM statistical descriptor (contrast) for all three samples. The intensity of variability can be observed by the range for each sample, where sample A is mineralogically the most homogeneous, hence has a short range in comparison with samples B and C, which have a broader range indicative of mineralogical variability

Developing a 3D mineral texture quantification method of drill core for geometallurgy

local variability in these transitions respectively. Correlation and energy refer to the probability of the occurrence of any specified pixel pair and the sum of the squared elements in the GLCM, respectively. These four statistical descriptors were calculated for the 3D volumes of each sample. As an example, the descriptive statistics for the contrast descriptor are summarized in Table I and a supporting box-and-whisker plot is illustrated in Figure 5.

The range of these contrast values for a specific sample is indicative of the intensity of the sample's variability, where shorter ranges are indicative of higher homogeneity in comparison with broader ranges, which are indicative of higher mineralogical variability. For example, sample A, has the shortest range (70 298–70 549), and is thus the most homogenous sample. The polymetallic samples, which have broader ranges (68 487–71 375 or 71 004–75 380 respectively), have higher mineralogical variability. However, the polymetallic ores (samples B and C) are distinguishable from each other, as reflected by their variability in mineralogy.

The contrast values can potentially also discriminate between textural features, where the higher positions (*i.e.* visually on the box-and-whisker plot as well as higher values) are indicative of coarser-grained rocks in comparison with finer grained rocks, which would have lower contrast values. However, the XCT analysis does not standardize the grey levels between different samples and hence the grey levels shown in Figure 4 -A1 are actually stretched in relation to Figures 4 -B1 and 3 -B2. While the statistical differences given in Table I are a true reflection of the differences between the images shown, they are not a true reflection of the differences between the samples because of the lack of standardization between the XCT images. These differences are a true reflection of the differences seen in the grey scale images and hence attest to the robustness and viability of the GLCM in differentiating different mineralogies and textures. Future work should address finding appropriate means for XCT calibration so that image information is directly comparable across rocks with different mineralogies.

Quantification of rock strength

Figure 6 shows examples of the true stress-true strain curves

for three pieces of the three samples (A, B, and C). The curves follow the conventional trend for compressive loading, whereby stress increases proportionally with strain until a peak value, beyond which it follows an unsteady decrease. The yield strength is the value at which stress begins to asymptote, representing a transition from elastic (reversible) to plastic (irreversible) deformation. The peak value of stress is known as the ultimate compressive strength (UCS), and represents the maximum stress the sample can resist before macroscopic fracture (Napier-Munn *et al.*, 1996). For sample A, the yield strength is distinct from the UCS, such that some plastic damage takes place prior to complete fracture. For samples B and C, fracture occurs immediately following the point of the initial yield.

Sample A has an average yield strength of 180 MPa, with a standard error of 29.1 MPa at the 95% confidence level. Samples B and C have average values of 104 MPa and 80 MPa, with standard errors of 12.4 and 25.9 MPa respectively. This signifies that sample A has a significantly higher yield strength than samples B and C, which have statistically similar strengths.

The Young's modulus is calculated as the gradient of the stress-strain curve over the elastic interval (King, 2001). This value is an indication of a material's susceptibility to deformation under load, where a higher value indicates a higher resistance to elastic behaviour. The average Young's moduli of the three samples were 60.7 ± 3.2 GPa (sample A), 50.6 ± 2.2 GPa (sample B), and 53.9 ± 1.9 GPa (sample C), with all errors calculated at 95% confidence level. The results indicate that of the three samples, the shale (sample A) deforms the least prior to fracture. Values obtained for the yield stress and Young's moduli were consistent with those reported in prior work on compression tests using these ores (Bbosa, 2007; Hill *et al.*, 2018).

Discussion

A key part of geometallurgy includes small-scale testing to capture the ore properties and define their inherent variability, which can potentially be used in geometallurgical proxies and block models. This becomes important in ore breakage characterization studies, especially when the ore feed to the comminution circuit is variable, as this can cause throughput

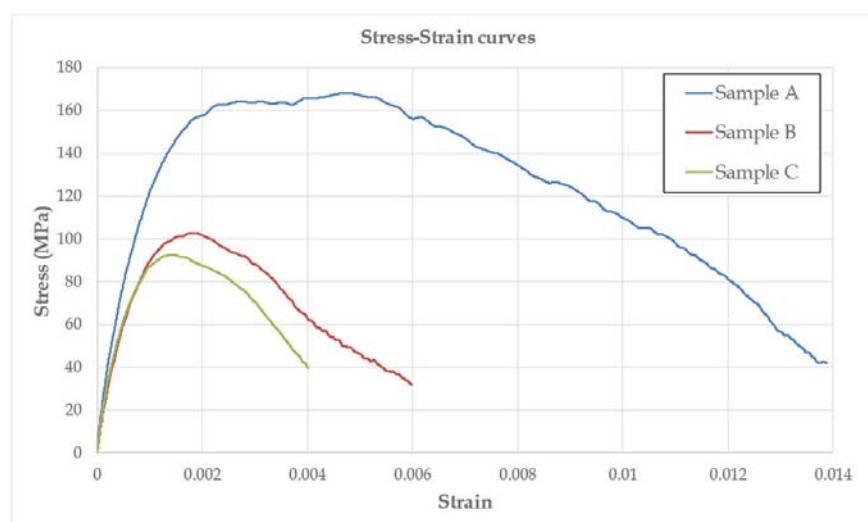


Figure 6—SHPB true stress-true strain curves using one example from each of the mineral texture types, *i.e.* shale (sample A) against the two different polymetallic ore samples (B and C)

Developing a 3D mineral texture quantification method of drill core for geometallurgy

fluctuations (Napier-Munn *et al.*, 1996). Through the opportunity that the 3D GLCM and XCT quantification method provides, not only can the textural variation be captured (fine vs. coarse), but also basic mineralogical information. This basic mineral texture capturing has been demonstrated in this study, and the results are as follows.

Sample A is a homogeneous shale consisting predominantly of quartz, feldspar, and micas in a fine-grained matrix. The GLCM heat map distribution confirms the mineralogy and texture through the broad distribution of pixel data in the top left (low-density) quadrant (see Figure 4), which indicates a fine-grained texture dominated by silicates. The GLCM statistics further show a clear trend distinct from the polymetallic ore: sample A has lower values for contrast and correlation, and higher values for energy and homogeneity. Sample A has a yield stress of 180 MPa and has the highest resistance to deformation.

Samples B and C are polymetallic sulphide ores, with a medium-grained matrix dominated by magnetite and quartz. There are subtle differences in their gangue and sulphide mineralogies. Sample B is dominated by pyroxmangite and chalcopyrite, whereas sample C is mostly sphalerite. The GLCM shows narrower distributions for both samples, which also indicates that these samples are more medium-grained in comparison with the finer grained shale. Sample C furthermore show a peak for the sulphides in the bottom right quadrant, indicative of high-density materials (Figure 4 -C3). If sulphides are not present in the grey level image (*e.g.* sample B), the bottom right quadrant will show no information (Figure 4-B3). The GLCM statistics show similar values for these two samples. Both samples B and C have a lower yield strength than the shale.

In this study, the XCT-GLCM method has been applied across two different sample sets to allow the evaluation of the sensitivity of the method to inter-sample variability. The work of Jardine, Becker, and Miller (2018) was limited to samples from a Ni-Cu sulphide ore, and thus did not allow such an evaluation. An important consideration that has emerged through this exercise is that the XCT grey level volumes of samples with very different mineral textures need to be directly comparable with one another, *i.e.* equivalent absolute grey levels will be measured for the same mineral regardless of its mineral matrix. This requires an internal calibration step which is, however, not routine practice in XCT scanning, as evidenced by comparison to the QEMSCAN BSE image (which has a BSE calibration step). Further development should investigate this as a routine step in the application of the method.

A further limitation in this study is the small sample set used. Validation for this work includes QEMSCAN analysis; however, it is not envisaged that the final stages of the 3D mineral texture quantification method will be dependent on QEMSCAN analysis. As demonstrated, the three mineral textural types can be used as building blocks for ongoing research towards the development of a correlation between mineral texture and rock strength using this 3D XCT and GLCM method. Additionally, the GLCM statistical descriptors do show sensitivity to variations in the data-set, and can potentially be used as an indicator of ore variability. Building such basic relationships can improve the management of ore heterogeneity, which is the essence of geometallurgy. Ideally, geometallurgical proxies should be developed and integrated with exploration, where the real need is in core logging systems. Since thousands of metres of core are routinely logged, these

proxies can predict processing response months or even years ahead of actual processing. Future work should therefore include incorporating the integral mineral composition and rock strength into potential textural descriptors by continuing testing.

Conclusions and recommendations

Mineral texture is a key parameter in geometallurgy, as is finding appropriate means to quantify it. As part of ongoing research (Becker *et al.*, 2016; Jardine, Becker, and Miller, 2018), this study advances the development of the method for 3D mineral texture quantification by comparing a heterogeneous polymetallic ore with a homogeneous shale. The current method provides a representation of drill core samples and captures the mineral textures through GLCM heat maps and statistical descriptors. The study demonstrated the use of the GLCM statistical descriptors, which potentially capture meaningful information for future quantification, as the complementary 3D GLCM heat map distributions are more graphical outputs. The study also demonstrated that the differences include the capturing of inherent properties, *i.e.* strength. Future work will include not only further testing of the polymetallic ore sample set, but also investigations of the underlying scientific principles of how the 3D quantification method captures the mineral textural variations, and the robustness of the method. The robustness investigation will include testing the quality of the 3D GLCM outputs for different XCT scanning conditions and methods for standardization between different ore types. Additionally, an understanding of the primary factors that contribute to the mineral texture and rock strength relationship is needed.

Acknowledgements

This work is based on research supported in part by the National Research Foundation of South Africa (grant numbers 86054, 99005). Any opinions, findings, and conclusions or recommendations expressed in any publication generated by NRF-supported research are those of the author(s), and the NRF accepts no liability whatsoever in this regard. This work is also supported through the South African Minerals to Metals Research Institute and the Department of Science and Technology. The authors would like to thank Lunga Bam at the Nuclear Energy Corporation South Africa and the rest of the MIXRAD laboratory team for their collaboration in the X-ray computed tomography studies. Gaynor Yorath and the QEMSCAN laboratory team are also acknowledged. Henry Gordon is especially thanked for supplying the appropriate samples.

References

- BAM, L.C., MILLER, J.A., BECKER, M., DE BEER, F.C., and BASSON, I. 2016. X-ray Computed Tomography: determination of rapid scanning parameters for geometallurgical analysis of iron ore. *Proceedings of the Third AusIMM International Geometallurgy Conference*, Perth, Western Australia, 15–17 June 2016. Australasian Institute of Mining and Metallurgy, Melbourne. pp. 209–220.
- BAUM, W. 2013. Ore characterization, process mineralogy and lab automation a roadmap for future mining. *Minerals Engineering*, vol. 60. pp. 69–73.
- BBOSA, L. 2007. Measurement of impact breakage properties of ore particles using a series of devices. MSc thesis, University of Cape Town.
- BECKER, M., JARDINE, M., MILLER, J.A., and HARRIS, M. 2016. X-ray Computed

Developing a 3D mineral texture quantification method of drill core for geometallurgy

- Tomography: A geometallurgical tool for 3D textural analysis of drill core? *Proceedings of the Third AusIMM International Geometallurgy Conference*, Perth, Western Australia, 15–17 June 2016 Australasian Institute of Mining and Metallurgy, Melbourne. pp. 15–16.
- CRAIG, J.R. and VAUGHAN, D.J. 1994. Ore Microscopy and Ore Petrography. 2nd edn. Mineralogical Society of America. http://www.minsocam.org/msa/OpenAccess_publications/Craig_Vaughan/
- EVANS, C.L., WIGHTMAN, E.M., and YUAN, X. 2015. Quantifying mineral grain size distributions for process modelling using X-ray micro-tomography. *Minerals Engineering*, vol. 82. pp. 78–83.
- GASPAR, O. and PINTO, A. 1991. The ore textures of the Neves Corvo volcanogenic massive sulphides and their implications for ore beneficiation. *Mineralogical Magazine*, vol. 55. pp. 417–422.
- GHOORBANI, Y., BECKER, M., PETERSEN, J., MAINZA, A.N., and FRANZIDIS, J.P. 2013. Investigation of the effect of mineralogy as rate-limiting factors in large particle leaching. *Minerals Engineering*, vol. 52. pp. 38–51.
- GHOORBANI, Y., BECKER, M., PETERSEN, J., MORAR, S.H., MAINZA, A., and FRANZIDIS, J.P. 2011. Use of X-ray computed tomography to investigate crack distribution and mineral dissemination in sphalerite ore particles. *Minerals Engineering*, vol. 24. pp. 1249–1257.
- GOTTLIEB, P., WILKIE, G., SUTHERLAND, D., HO-TUN, E., SUTHERS, S., PERERA, K., JENKINS, B., SPENCER, S., BUTCHER, A., and RAYNER, J. 2000. Using quantitative electron microscopy for process mineralogy applications. *JOM*, vol. 52, no. 4. pp. 24–25.
- GOVENDER, R.A., LOUCA, L.A., PULLEN, A., FALLAH, A.S., and NURICK, G.N. 2012. Determining the through-thickness properties of thick glass fiber reinforced polymers at high strain rates. *Journal of Composite Materials*, vol. 46. pp. 1219–1228.
- HARALICK, R.M., SHANMUGAM, K., and DINSTEN, I. 1973. Textural features for image classification. *Transactions on Systems and Cybernetics*, vol. 3. pp. 610–621.
- HILL, H., MAINZA, A., BBOSA, L., and BECKER, M. 2018. Comparing the ore breakage characteristics of drill core and crushed ore using the JKRB. *Proceedings of the XXIX International Mineral Processing Council Conference*, Moscow, 15–21 September.
- HOWARTH, D.F. and ROWLAND, J.C. 1987. Quantitative assessment of rock texture and correlation with drillability and strength properties. *Rock Mechanics and Rock Engineering*, vol. 20. pp. 61–84.
- JARDINE, M., BECKER, M., and MILLER, J. A. 2018. Coupled X-ray computed tomography and grey level co-occurrence matrices as a method for quantification of mineralogy and texture in 3D. *Computers and Geosciences*, vol. 111. pp. 105–117.
- KING, R.P. 2001. Modeling and Simulation of Mineral Processing Systems. Butterworth-Heinemann.
- LITTLE, L., MAINZA, A.N., BECKER, M., and WIESE, J. 2016. Using mineralogical and particle shape analysis to investigate enhanced mineral liberation through phase boundary fracture. *Powder Technology*, vol. 301. pp. 794–804.
- LOTTER, N.O. 2011. Modern process mineralogy: An integrated multi-disciplined approach to flowsheeting. *Minerals Engineering*, vol. 24, no. 12. pp. 1229–1237.
- LOTTER, N.O., KORMOS, L.J., OLIVEIRA, J., FRAGOMENI, D., and WHITEMAN, E. 2011. Modern process mineralogy: two case studies. *Minerals Engineering*, vol. 24. pp. 638–650.
- LUND, C., LAMBERG, P., and LINDBERG, T. 2013. Practical way to quantify minerals from chemical assays at Malmberget iron ore operations, an important tool for the geometallurgical program. *Minerals Engineering*, vol. 49. pp. 7–16.
- LUJ, W., PAWLIK, M., and LASKOWSKI, J. 2015. The role of colloidal precipitates in the interfacial behaviour of alkyl amines at gas-liquid and gas-liquid-solid interfaces. *Minerals Engineering*, vol. 72. pp. 47–56.
- MARIANO, R.A. 2016. Measurement and modelling of the liberation and distribution of minerals in comminuted ores. PhD, thesis, University of Queensland.
- MAYDAGAN, L., FRANCHINI, M., IMPICINI, A., and LENTZ, D. 2016. Phyllosilicates geochemistry and distribution in the Altar porphyry Cu-(Au) deposit, Andes Cordillera of San Juan, Argentina: Applications in exploration, geothermometry, and geometallurgy. *Journal of Geochemical Exploration*, vol. 167. pp. 108–109.
- MCGRATH, T.D.H., O'CONNOR, L., and EKSTEEN, J.J. 2015. A comparison of 2D and 3D shape characterisations of free gold particles in gravity and flash flotation concentrates. *Minerals Engineering*, vol. 82. pp. 45–53.
- MILLER, J.D. and LIN, C.L. 2016. Opportunities for plant-site 3D coarse particle characterization with automated high-speed X-ray tomography. *Proceedings of the 2016 SME Annual Conference and Expo: The Future for Mining in a Data-Driven World*, Phoenix, AZ, 21–24 February 2016. pp. 811–814.
- NAPIER-MUNN, T.J., MORRELL, S., MORRISON, R.D., and KOJOVIC, T. 1996. Mineral Comminution Circuits: their Operation and Optimisation. 6th edn. Julius Kruttschnitt Mineral Research Centre, University of Queensland, Brisbane, Australia.
- NGUYEN, K. 2013. A new texture analysis technique for geometallurgy. *Proceedings of the Second AusIMM International Geometallurgy Conference*, Brisbane, 30 September - 2 October 2013. Australasian Institute of Mining and Metallurgy, Melbourne. pp. 187–190.
- NWAILA, G. 2014. Application of HPGR and X-ray CT to investigate the potential of Witwatersrand gold ore for heap leaching: A process mineralogy approach. MSc thesis, University of Cape Town.
- OLSSON, W.A. 1974. Grain size dependence of yield stress in marble. *Geophysics*, vol. 79, no. 32. pp. 4859–4861.
- PARBHAKAR-FOX, A.K., EDRAKI, M., WALTERS, S., and BRADSHAW, D. 2011. Development of a textural index for the prediction of acid rock drainage. *Minerals Engineering*, vol. 24. pp. 1277–1287.
- PEREZ-BARNEVO, L., LÉVESQUE, S., and BAZIN, C. 2018. Automated recognition of drill core textures: A geometallurgical tool for mineral processing prediction. *Minerals Engineering*, vol. 118. pp. 87–96.
- POWELL, M.S. 2013. Utilising orebody knowledge to improve comminution circuit design and energy utilisation. *Proceedings of the Second AusIMM International Geometallurgy Conference*, Brisbane, 30 September - 2 October 2013. Australasian Institute of Mining and Metallurgy, Melbourne. pp. 27–35.
- SCHOUWSTRA, R. and SMIT, A.J. 2011. Developments of mineralogical techniques. *Minerals Engineering*, vol. 24, no. 12. pp. 1224–1228.
- SCHOUWSTRA, R., DE VAUX, D., MUZONDO, T., and PRINS, C. 2013. A geometallurgical approach at Anglo American Platinum's Mogalakwena operation. *Proceedings of the Second AusIMM International Geometallurgy Conference*, Brisbane, 30 September - 2 October 2013. Australasian Institute of Mining and Metallurgy, Melbourne. pp. 85–92.
- TAVARES, L.M. and KING, R.P. 1998. Single-particle fracture under impact loading. *Mineral Processing*, vol. 54, no. 1. pp. 1–28.
- TUNGPALAN, K., MANLAPIG, E., ANDRUSIEWICZ, M., KEENEY, L., WIGHTMAN, E., and EDRAKI, M. 2015. An integrated approach of predicting metallurgical performance relating to variability in deposit characteristics. *Minerals Engineering*, vol. 71. pp. 49–54.
- VIZCARRA, T.G., WIGHTMAN, E.M., JOHNSON, N.W., and MANLAPIG, E.V. 2010. The effect of breakage mechanism on the mineral liberation properties of sulphide ores. *Minerals Engineering*, vol. 23. pp. 374–382.
- VOS, F. 2016. The effect of mineral grain textures at particle surfaces on flotation response. PhD thesis, University of Queensland.
- YILDIRIM, B.G., BRADSHAW, D., POWELL, M., EVANS, C., and CLARK, A. 2014. Development of an effective and practical Process Alteration Index (PAI) for predicting metallurgical responses of Cu porphyries. *Minerals Engineering*, vol. 69. pp. 91–96. ◆